https://doi.org/10.5194/egusphere-2024-1256
Preprint. Discussion started: 17 May 2024


# What Are the Key Soil Hydrological Processes to Control Soil Moisture Memory?

**Mohammad A. Farmani[1], Ali Behrangi[1,2], Aniket Gupta[1], Ahmad Tavakoly[3,4], Matthew Geheran[3], and Guo-Yue Niu[1]**

[1]Department of Hydrology and Atmospheric Sciences, University of Arizona, Tucson, AZ, USA,
[2]Department of Geosciences, University of Arizona, Tucson, AZ, USA,
[3]US Army Engineer Research and Development Center, Coastal and Hydraulics Laboratory, Vicksburg, MS, USA,
[4]Earth System Science Interdisciplinary Center, University of Maryland, College Park, MD, USA

Corresponding author: Mohammad Farmani, email: farmani@arizona.edu
Guo-Yue Niu, email: niug@arizona.edu

**Key Points:**

- Van-Genuchten soil hydraulics significantly affect the long-term Soil Moisture Memory (SMM) of topsoil.
- Surface ponding enhances surface soil moisture in both topsoil and the root zone.
- Enhanced infiltration through preferential pathways improves both short-term and long-term SMM in both topsoil and the root zone.

https://doi.org/10.5194/egusphere-2024-1256
Preprint. Discussion started: 17 May 2024


## Abstract

Soil moisture memory (SMM), which refers to how long a perturbation in Soil Moisture (SM) can last, is critical for understanding climatic, hydrologic, and ecosystem interactions. Most land surface models (LSMs) tend to overestimate surface soil moisture and its persistency, sustaining unexpectedly large soil surface evaporation. In general, LSMs show an overestimation of long-term SMM and an underestimation of short-term SMM. This study aims to 1) identify key soil hydrological/hydraulic processes that contribute to the amount and persistence of SM and 2) improve the physical representations of soil hydrology in the widely-used Noah-MP LSM with optional schemes of soil hydrology/hydraulics. We test the effects of different processes on SMM, including soil water retention characteristics (or soil hydraulics), soil permeability, and surface ponding. We compare SMMs computed from various Noah-MP configurations against that derived from the Soil Moisture Active Passive (SMAP) Level 3 soil moisture and in-situ measurements from the International Soil Moisture Network (ISMN) from year 2015 to 2019 over the contiguous United States (CONUS). The results suggest that 1) soil hydraulics plays a dominant role, and the Van-Genuchten hydraulic scheme reduces the overestimation of the long-term surface SMM produced by the Brooks-Corey scheme, which is commonly used in LSMs; 2) explicitly representing surface ponding improves SMM accuracy for both the surface layer and the root zone; and 3) enhanced permeability through macropores improves the overall representation of soil hydraulic dynamics. The combination of schemes introduced in this study can significantly improve the long-term memory overestimation and short-term memory underestimation issues in LSMs.

https://doi.org/10.5194/egusphere-2024-1256
Preprint. Discussion started: 17 May 2024


## Plain Language Summary

Land surface models (LSMs) represent the physical and bio-geochemical exchanges of mass and energy between surface and atmosphere. Such exchanges are extensively dependent on the surface soil moisture amount and its persistence. This study explores the key hydrological processes that can improve the representation of soil water holding and release capacity in land surface models, which are important for weather and climate predictions. Through experiments with state-of-the-art model, we found that soil hydraulics (representing how efficiently soil can hold/release water under variable pressure) is particularly effective in sustaining soil moisture. Additionally, we found that allowing water to pond on the soil surface helps improve the model's soil moisture persistency. Furthermore, enhanced soil permeability representation through soil macropores also regulates the water movement hence improving the soil moisture persistency. Overall, the combination of the above-mentioned approaches significantly improves the model's accuracy in representing how quickly the soil dries out and how efficiently it retains the moisture.

https://doi.org/10.5194/egusphere-2024-1256
Preprint. Discussion started: 17 May 2024


# 1. Introduction

LSM efficacy in simulating climate feedback mechanisms critically depends on the soil retention capacity and soil moisture persistency. Rainwater that rapidly infiltrates into deeper subsoil strata is unavailable to be returned to the atmosphere through evaporation, thereby preventing potential atmospheric feedback loops (Mccoll et al., 2019). The influence of soil moisture on climate predictions at seasonal-to-sub-seasonal (S2S) scales is well-recognized due to its role in the exchange of surface energy and water fluxes with the atmosphere (Koster et al., 2002, 2010; Koster, Guo, et al., 2009; Koster & Suarez, 2001). Water stored in soil and aquifers, which variably persists from seasons to years, is known to affect precipitation variability (Koster & Suarez, 1999, 2001). This impact is particularly pronounced in regions transitioning from dry to wet conditions, where evapotranspiration (ET) is highly sensitive to soil moisture levels (Guo et al., 2006; Koster et al., 2004; Koster & Suarez, 2001; Seneviratne, Koster, et al., 2006). While the nature and scale of soil moisture-precipitation feedback are still being debated (Findell et al., 2011; Taylor et al., 2013), numerous studies have emphasized the importance of soil moisture initialization and its persistency for accurate climate predictions (Dirmeyer, 2011; Mei & Wang, 2012; Tuttle & Salvucci, 2016; Zeng et al., 2010). The degree of soil moisture-precipitation coupling widely varies across different climate models (Koster et al., 2004; Koster & Suarez, 1999, 2001; Moghisi et al., 2024; Seneviratne & Koster, 2012; Taylor et al., 2012), and discrepancies in the modeled soil moisture by Land Surface Models (LSMs) for climate modeling are notable (A. Boone, 2004).

Refinement of soil moisture-precipitation feedback in LSMs is hindered by the lack of large-scale observational data, challenging the improvement and validation of simulations (Koster et al., 2010; Koster & Mahanama, 2012; Koster & Suarez, 1999, 2001; Seneviratne & Koster, 2012). This shortfall highlights the necessity for more detailed representations of land-atmosphere feedback mechanisms that are crucial for extreme weather event predictions, yet are typically parameterized rather than explicitly resolved in models (Mccoll et al., 2019; Pastorello et al., 2020). Integrating extensive observational data is vital for simulating the intricacies of climate and weather and improving model predictive skill (Koster et al., 2017; Koster, Schubert, et al., 2009a; Mccoll et al., 2019; Shellito et al., 2018). Recent advancements in remote sensing observations have enabled analyses of interactions between near-surface soil and the atmosphere. Nonetheless, the paucity of root zone data complicates the investigation of deep soil dynamics. Numerous studies have utilized satellite soil moisture products to evaluate and refine models, focusing on the spatial and temporal patterns of soil moisture variability (Koster, Schubert, et al., 2009b; K. Yang et al., 2020). In particular, the Soil Moisture Active Passive (SMAP) mission has been extensively employed to assess model performance (Mccoll et al., 2019; McColl, Wang, et al., 2017a, 2017b; Shellito et al., 2016, 2018).

The concept of Soil Moisture Memory (SMM)— the duration required for a perturbation, such as rainfall, to dissipate—becomes essential for understanding the land-atmosphere interactions. SMM encapsulates the temporal variations of soil moisture, reflecting the exchange of fluxes between land and atmosphere. Therefore, SMM is an important metric for evaluating LSMs, since one of their functions is to provide flux exchange and boundary conditions for atmospheric models (Guo et al., 2006; Koster et al., 2004; Koster, Schubert, et al., 2009a; Seneviratne, Koster, et al., 2006). SMM also facilitates the comparison of how quickly soil loses water between observations and various models, providing insights into the mechanisms within LSMs and their

https://doi.org/10.5194/egusphere-2024-1256
Preprint. Discussion started: 17 May 2024


hydrometeorological responses. Moreover, analyzing SMM can yield valuable data on the configurations and hydrological parameterizations of specific LSMs, thus improving our understanding of how different configurations impact model performance, particularly in soil moisture representation. Shellito et al. (2018) measured the drying rate of surface soil moisture, which they considered as soil moisture memory, using SMAP data and the Noah model during the initial 1.8 years following SMAP's launch. They concluded that SMAP has faster drying rate compared with Noah.

Determining SMM is not straightforward due to the variety of calculation methods proposed by researchers (Ghannam et al., 2016; Katul et al., 2007; Koster et al., 2002, 2004; Koster, Guo, et al., 2009; Koster & Suarez, 1999, 2001; Mao et al., 2020; McColl, Alemohammad, et al., 2017; Mccoll et al., 2019; McColl, Wang, et al., 2017a; Seneviratne, Koster, et al., 2006; Shellito et al., 2016), each introducing its own level of uncertainty. Traditionally, soil moisture has been conceptualized as a red noise process, forming the basis for SMM calculations (T. L. Delworth & Manabe, 1988). This approach has led to the definition of SMM as the e-folding autocorrelation timescale within such a process (T. Delworth & Manabe, 1989). SMM has also been characterized using various other autocorrelation-based methods, such as the integral timescale (Ghannam et al., 2016; Nakai et al., 2014), soil moisture variance spectrum (Katul et al., 2007; Nakai et al., 2014), and the constant time lag autocorrelation (Koster & Suarez, 2001; Seneviratne, Lüthi, et al., 2006). These methods provide insights into the magnitudes of water and energy flux exchanges between land surface and atmosphere, indicating that shorter SMM durations can lead to more intense feedback and larger flux exchanges. Traditionally, these models were applied to monthly datasets. However, this approach risks overlooking dynamic processes governed by limitations in water and energy (Mccoll et al., 2019). Consequently, there has been a shift away from their use towards recent high-resolution observational and modeling data. Therefore, there is a need for further research to refine SMM measurement that can then be used as a benchmark for assessing LSMs (Mccoll et al., 2019).

McColl et al. (2019) categorized soil water loss into two main categories: water-limited (long-term) and energy-limited (short-term). The energy-limited regime is a process where water loss is constrained by available energy and lasts from hours to a few days. In contrast, the water-limited regime is a process where water loss depends on the available water and spans longer periods, such as weeks, months, and seasons. McColl et al. (2019) specified that ET and drainage are the main controllers of long-term and short-term memories, respectively. Utilizing a two-year dataset from the SMAP mission and simulations from the Goddard Earth Observing System Model, Version 5 (GEOS-5), McColl et al. (2019) conducted a global analysis under various climatic and land conditions. Their analysis revealed that GEOS-5 tends to overpredict the duration of water-limited memory and underpredicts energy-limited memory compared to SMM inferred from SMAP data, while the results were not affected by the SMAP sampling frequency of 3 days. Building on this, He et al. (2023) employed the hybrid memory approach proposed by McColl et al. (2019) to assess the hydrometeorological response of various LSMs, including GLDAS-CLSM, GLDAS-Noah, MERRA2, NCEP, ERA5, and JRA55, against SMAP observations for 2015 – 2020. The authors observed that LSMs generally overestimate memory in water-limited regime and significantly underestimate it in energy-limited regime. Moreover, their study suggested that discrepancies in SMM representation within LSMs are more attributable to the physical processes incorporated rather than factors such as soil layer depth or the nature of model simulations (online/offline).

https://doi.org/10.5194/egusphere-2024-1256
Preprint. Discussion started: 17 May 2024


Based on the works of McColl et al. (2019) and He et al. (2023), this study examines subsurface processes to enhance the Noah-MP model's parametrization, focusing on SMM as a key metric. We aim to optimize soil hydraulics within the model by evaluating various parametrizations, such as those by Brooks and Corey (1964), Clapp and Hornberger, and Van-Genuchten, along with considering preferential flow and surface ponding depth. Our analysis investigates the impact of these configurations on soil moisture consistency across different ET regimes and drainage, so it provides insight into physical processes affecting SMM. By comparing SMM in Noah-MP with SMAP Level 3 data and ISMN observations from 2015 to 2019 over the CONUS, we seek to refine parametrization schemes and address prevalent SMM overestimations in LSMs.

## 2. Materials and Methods

SMM denotes the duration required for a perturbation to dissipate, or the period from the start to the end of a perturbation. For instance, following precipitation, the change in near-surface soil moisture marks the beginning of the perturbation. This excess moisture gradually diminishes due to flux exchange or percolation to deeper soil layers. The moisture level of soil plays a critical role in influencing water loss patterns. Following rainfall, the upper layer of soil initially holds more moisture than its field capacity ($\theta_{fc}$), causing runoff and drainage (see Figure 1a). Subsequently, as the soil gradually dries, its moisture content reduces to a range between $\theta_{fc}$ and the critical threshold ($\theta_c$). This phase leads to consistent water loss at the maximum evapotranspiration rate, known as Stage-I ET. As this process continues, the soil moisture falls below $\theta_c$ (Figure 1a), at which stage evapotranspiration becomes limited by the available water, termed Stage-II ET or ET at water-limited regime (illustrated in Figure 1a & b). Ultimately, when the soil moisture drops below the wilting point ($\theta_w$), water no longer leaves the soil. Therefore, the whole process of water loss depends on the soil's moisture level and falls into two main types: energy-limited including unresolved drainage, and Stage-I ET, and water-limited including Stage-II ET (Figure 1b) (Mccoll et al., 2019; He et al. 2023). Energy-limited, green strips, and water-limited regimes, dotted-lines, are shown in soil moisture times series at the Tonzi Ranch station (Figure 1c).

https://doi.org/10.5194/egusphere-2024-1256
Preprint. Discussion started: 17 May 2024


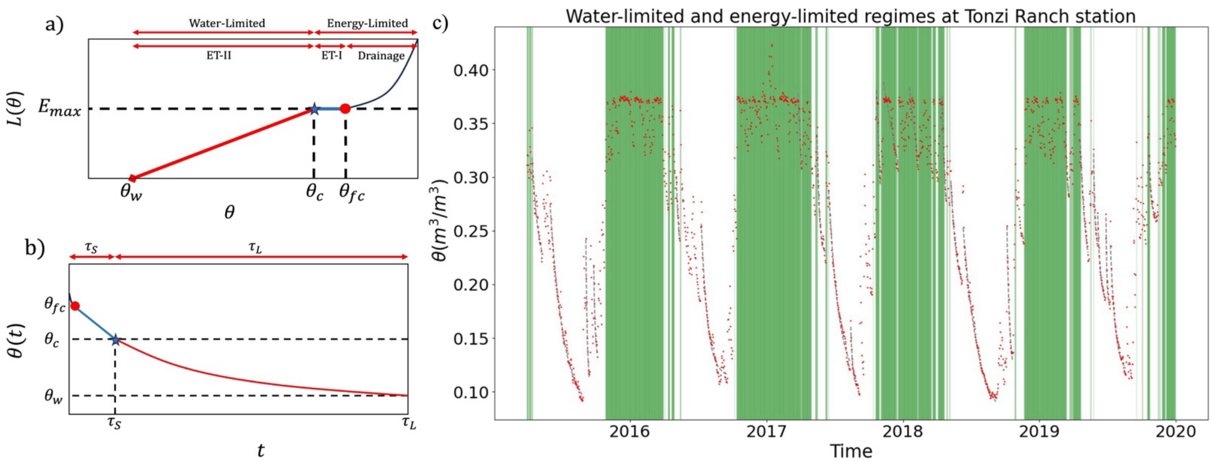


Figure 1 Schematic diagrams of (a) surface water loss process and (b) soil moisture memory at different soil moisture regimes [adapted from (McColl, Wang, et al., 2017b)]. Note that the x-axis in (a) refers to soil moisture ($m^3m^{-3}$), and y-axis refers to surface water loss rate, L($\theta$) (mm/s); $E_{max}$ is the maximum evaporation rate (mm/s ). In (b), x-axis refers to time (e.g., days) and y-axis to SM content ($m^3m^{-3}$). Panel (c) shows the SM time series for the Tonzi Ranch station, with green periods indicating energy-limited regime and dotted lines representing water-limited regime. $\theta_c$, and $\theta_{fc}$ refer to the wilting point, critical point, and field capacity, respectively.

### 1.1 Soil Moisture Memory of Water-Limited Regime ($\tau_L$) and Energy-Limited Regime ($\tau_S$)

McColl et al. (2019) considered the SMM concept as it relates to two regimes: a) the memory of water-limited regime ($\tau_L$), specified by 'L' abbreviation of Long-term, b) the memory of energy-limited regime ($\tau_S$), specified by 'S' abbreviation of Short-term. Their model incorporates a deterministic equation to represent water-limited processes during soil moisture drydown periods. However, energy-limited processes occur over shorter timescales and present a challenge for current satellite technologies to provide precise observations. McColl et al. (2019) highlighted that drainage is not a completely resolved process by satellite observations. To address this gap, McColl et al. (2019) proposed a stochastic equation to capture the unresolved nature of energy-limited processes.

The hybrid model is formulated by McColl et al. (2019) as follows:

$$\frac{d\theta(t)}{dt} = \begin{cases} \dfrac{-\theta(t) - \theta_w}{\tau_L}, P = 0 \\ \dfrac{-\theta(t) - \overline{\theta}}{\tau_S} + \varepsilon(t), P > 0 \end{cases} \quad (1)$$

where, $\theta$ is the volumetric soil moisture, P indicates precipitation, $\theta_w$ is the minimum soil moisture, $\overline{\theta}$ is the time-averaged SM, and $\varepsilon(t)$ is a random variable with a mean of zero. $\tau_L$ and $\tau_S$ are SMM

https://doi.org/10.5194/egusphere-2024-1256
Preprint. Discussion started: 17 May 2024


for the water-limited and energy-limited regimes, respectively. McColl et al. (2019) solved these equations, demonstrating that the memories can be expressed as:

$$\theta(t) = \Delta\theta exp\left(\frac{-t}{\tau_L}\right) + \theta_w P = 0 \quad (2)$$

$$\tau_S = \frac{-\frac{\Delta t}{2}}{log} \quad (3)$$

$\Delta\theta$ represents the soil moisture changes during drydown, $\Delta t$ is the temporal resolution of the soil moisture data, $\alpha$ is the precipitation intensity, $\Delta z$ is soil layer thickness, and $\overline{\Delta\theta_+} = \theta(\mathrm{t}) - \theta(\mathrm{t} - \Delta\mathrm{t})$ represents a positive increment in soil moisture. McColl et al. (2017a) defined $\frac{\Delta z\,\overline{[\Delta\theta_+]}}{\alpha}$ as stored fraction of precipitation, indicating the average proportion of water that still exists in soil layer $\Delta t$ days after rainfall. McColl et al. (2019) declared that the short-term memory in their hybrid model is dominated by drainage when the sampling is relatively high (as in the case of SMAP's sampling frequency of 3 days). This approach and its rationale are further elaborated in McColl et al. (2017a) and McColl et al. (2019).

In the analysis of water-limited memory, we fitted Equation 2 to the soil moisture time series during specific drydown intervals. Then, $\tau_L$ was extracted as a parameter from the fitting curve (black dotted lines in Figure 1c). In contrast, short-term memory was determined directly using Equation 3, as indicated by the green periods in Figure 1c. Further information about the criteria for calculating memories can be found in McColl et al. (2019).

## 1.2 Description of Datasets

We use high-resolution atmospheric forcing datasets to drive the Noah-MP LSM. This model is set up to simulate soil moisture dynamics, featuring advanced infiltration and water retention processes. Additionally, it includes a precise parameterization for ponding depth. This setup facilitated five distinct experiments. Then, we used surface and root zone soil moisture data derived from the Noah-MP experiments, SMAP Level 3 surface soil moisture measurements, and root zone soil moisture measurements from the International Soil Moisture Network (ISMN) to calculate the hybrid SMM. The rest of this section describes in detail the forcing and observational datasets, the Noah-MP LSM configurations, the employed infiltration and water retention schemes, and the ponding depth threshold criterion.

### 1.2.1 Atmospheric Forcing, Soil and Vegetation Parameters

For modeling purposes, this study utilized the North American Data Assimilation System Phase 2 (NLDAS-2) near-surface meteorological data at an hourly interval and 0.125° spatial resolution.

https://doi.org/10.5194/egusphere-2024-1256
Preprint. Discussion started: 17 May 2024


This dataset encompasses a range of variables including air temperature, specific humidity, wind speed, surface pressure, shortwave and longwave radiation, and precipitation (Xia et al., 2012). We also used precipitation data from the Integrated Multi-satellite Retrievals for Global Precipitation Measurement (IMERG-Final) dataset (Huffman et al., 2020), which offers half-hourly measurements across a 0.1° grid extending from 60°S to 60°N. Subsequently, the IMERG-Final data were mapped to the 0.125° resolution of NLDAS-2 using bilinear interpolation. These precipitation data sources were integrated into the short-term SMM computation process.

To ascertain soil and vegetation parameters, the hybrid State Soil Geographic Database (STATSGO) with a 1-km resolution and the United States Geological Survey's (USGS) 24-category vegetation classification were employed. The datasets were aggregated to align with a 0.125° resolution, which is consistent with the NLDAS-2 forcing data. This process included determining the dominant soil and vegetation types for each grid cell. Subsequently, the lookup tables within the Noah-MP model (G. Niu et al., 2020) were used to assign the relevant parameters to the corresponding soil and vegetation categories.

### 1.2.2 SMAP L3 Surface Soil Moisture

Since its successful deployment on January 31, 2015, the Soil Moisture Active Passive (SMAP) observatory has consistently provided global volumetric soil moisture estimates every two or three days (Entekhabi et al., 2010). Its onboard radiometer, operating in the L-band frequency of the microwave spectrum, senses the top five centimeters of the soil column. In this study, we selected the SMAP Level 3 morning overpass due to the greater likelihood of air and surface temperature equilibrium during these hours, a critical condition for the SMAP retrieval algorithm. The L3 SMAP data used here span from 2015 to 2020, have a spatial resolution of 9 kilometers and are instrumental in calculating SMM across the Continental United States (CONUS).

In line with established methodologies from previous research (He et al., 2023; Mccoll et al., 2019), a quality control protocol was deemed necessary to refine soil moisture data in regions affected by dense vegetation, bodies of water, and permafrost, thereby mitigating noise present in satellite measurements (He et al., 2023; Mccoll et al., 2019; McColl, Wang, et al., 2017b). However, this study is conducted to determine SMM to deepen our knowledge of physical processes and to get closer to optimal soil hydraulic parametrizations within Noah-MP. This is achieved through a comparative analysis of SMM derived from SMAP and Noah-MP datasets. Given that a specific parametrization within Noah-MP has a pronounced impact on the eastern region of the Continental United States (CONUS)—a region that also corresponds with a significant portion of SMAP's low-quality data—we chose not to filter SMAP data to fully capture the parametrization effects within our study's geographical focus. This approach was intended to maintain consistency across figures and enhance the presentation of our findings. Furthermore, our objective is to showcase the physical process involved in SMM, rather than focusing on model accuracy in comparison with SMAP data. Note that the SMM maps from McColl et al (2019) and He et al (2023) demonstrated the effect of removing SMAP low-quality data, and hence we did not include the map of locations with high-quality SMAP data. Given that the surface water balance is sensitive to the temporal resolution of the analyzed surface soil moisture data, the SMAP L3 soil moisture data are resampled to achieve a consistent sampling frequency of one per three days at each pixel (He et al., 2023; McColl, Wang, et al., 2017a).

https://doi.org/10.5194/egusphere-2024-1256
Preprint. Discussion started: 17 May 2024


### 1.2.3 International Soil Moisture Network (ISMN)

In evaluating the Noah-MP model's parametrization for the root zone soil moisture, SMM is computed using both the model's outputs and in situ observations across the CONUS. We obtained the in situ soil moisture data from the International Soil Moisture Network (ISMN) portal (Dorigo et al., 2011), which compiles quality-controlled measurements from various sensors across multiple networks, Figure *2*. We exclude stations with less than 90% of their data rated as "good" quality. Despite the diversity of sensor types within ISMN, its stringent quality assurance protocols suggests that it is a reliable benchmark for validating soil moisture products (Colliander et al., 2017; Shellito et al., 2016). For the representation of root zone soil moisture, we select only the data from the top 1 meter of soil flagged as "good" quality. These measurements are averaged, i.e., hourly data aggregated to daily means, and the daily time series are used to compute both long-term and short-term SMM.

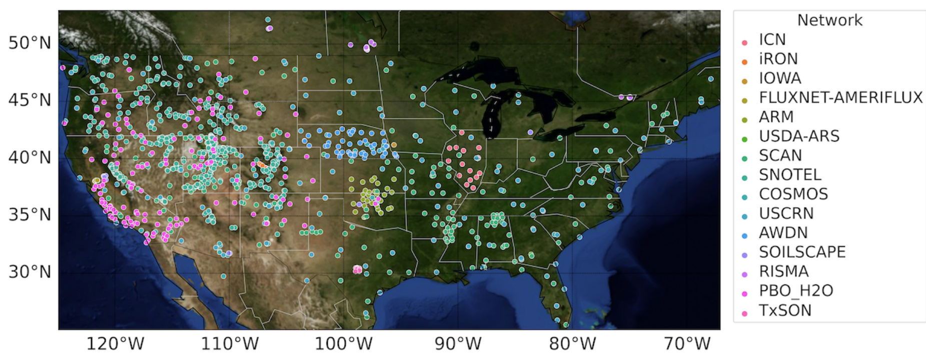


Figure 2 ISMN in-situ locations and networks over CONUS.

### 1.3 Noah-MP with Advanced Soil Hydrology

In this study, we choose Noah-MP (G. Y. Niu et al., 2011; Z.-L. Yang et al., 2011) for its extensive use within the Weather Research and Forecasting (WRF) model, the Unified Forecast System (UFS) for weather and short-term climate projections, and the National Water Model (NWM) for streamflow and water resource forecasting. The "semi-tile" sub-grid methodology of Noah-MP enables detailed calculation of surface energy and fluxes, differentiating effectively between bare and vegetated terrains to precisely compute variables such as latent and sensible heat fluxes (Agnihotri et al., 2023).

The Noah-MP version used in this study includes additional developments in plant hydraulics that explicitly represent plant water storage supplied by root water uptake driven by the hydraulic gradient between the soil and roots (G. Niu et al., 2020) and advanced soil hydrology that solves mixed-form Richards' equation and thus explicitly represents surface ponding, infiltration of surface ponded water, and preferential flow (Niu et al, 2024). As such, current Noah-MP accounts for water flow driven by the hydraulic gradients from the soil to the vegetation canopy to meet the

https://doi.org/10.5194/egusphere-2024-1256
Preprint. Discussion started: 17 May 2024


plant transpiration demand. It also accounts for subgrid variability in infiltration capacity through a fractional area of preferential flow pathways caused by soil macropores in the fields.

**The Mixed-Form Richards' Equation:** Most LSMs solve the mass-based (or θ-based) Richards' Equation (RE) for unsaturated soils (Chen & Dudhia, 2001; Oleson et al., 2010) and thus are not adequate to represent saturated conditions, e.g., surface ponding and groundwater dynamics. The current Noah-MP adopts the methodology of Celia et al. (1990) to solve the mass-pressure (θ-h) mixed-form RE (MF). The new solver solves pressure head, h, and conserves mass due to the mass (θ) constraint. To achieve a more accurate solution of $h$ and mass balance, the solver takes an adaptive time stepping scheme.

Surface ponding occurs when the pressure head of the surface layer is greater than the air entry pressure, and the upper boundary condition (BC) shifts from flux BC to head BC. Infiltration-excess runoff occurs when the surface ponding depth, $H_{top}$, surpasses a predefined threshold, $H_{top,max}$, at which the surface ponded water at local depressions of a model grid starts to be connected and runs off. The model extends its vertical domain to the bedrock depth (Pelletier et al., 2016) at which the lower boundary condition is set up as zero-flux. Groundwater discharge is represented using the TOPMODEL concept as a function of water table depth, which is determined by the modeled pressure head and interpolated.

**Optional Soil Hydraulics Schemes:** The current Noah-MP provides optional hydraulics schemes of the Van Genuchten-Mualem (VGM) and the Brooks-Corey with Clapp-Hornberger (BC/CH) parameters. To facilitate quicker convergence, particularly near saturation, we smoothed the BC/CH water retention curve using a polynomial function following Bisht et al. (2018).

**Representing Preferential Flow:** To represent preferential flow, current Noah-MP adopts a dual-permeability model (DPM) approach, partitioning the model grid into two domains: one representing rapid flow with reduced suction head (macropores) and the other for slower matrix flow, following Simunek and van Genuchten (2008) and Gerke and van Genuchten (1993a,b, 1996). This approach represents subgrid variability in infiltration capacity through a fractional area of soil macropores in the fields, $\mathbf{F}_a$, (or volumetric fraction of macropores). DPM also represents water transfer between the two pore domains, which can either be positive (lateral infiltration during rapid downward flow) or negative (diffusion from micropores to drier macropores). It also accounts for lateral movement of surface ponded water from the matrix to macropore domains at the soil surface. The aggregated water content (θ) and vertical water flux (q) for a grid cell are given by $\theta = F_a\, \theta_a + (1-F_a)\, \theta_i$, and $q = F_a\, q_a + (1-F_a)\, q_i$, respectively, where q denotes a water flux and the subscripts a and i respectively indicate macropore and micropore domains. This approach also extends to other water fluxes, such as $E_{soil}$ and groundwater recharge.

Table 1 Noah-MP Options used in this study.

| Process | Options | Schemes |
|---|---|---|
| Dynamic vegetation | DVEG = 2 | Dynamic vegetation |
| Canopy stomatal resistance | OPT_CRS = 1 | Ball-Berry type |
| Moisture factor for stomatal resistance | OPT_BTR = 1 | Plant water stress |

https://doi.org/10.5194/egusphere-2024-1256
Preprint. Discussion started: 17 May 2024


| | | |
|---|---|---|
| Runoff and groundwater | OPT_RUN = 1 | TOPMODEL with groundwater |
| Surface layer exchange coefficient | OPT_SFC = 1 | Monin-Obukhov similarity theory (MOST) |
| Radiation transfer | OPT_RAD = 1 | Modified two-stream |
| Ground snow surface albedo | OPT_ALB = 3 | Two-stream radiation scheme (Wang et al., 2022) |
| Precipitation partitioning | OPT_SNF = 5 | Wet bulb temperature (Wang et al., 2019) |
| Lower boundary condition for soil temperature | OPT_TBOT = 2 | 2-m air temperature climatology at 8m |
| Snow/soil temperature time scheme | OPT_STC = 1 | Semi-implicit |
| Surface evaporation resistance | OPT_RSF = 1 | Sakaguchi and Zeng (2009) |
| Root profile | OPT_ROOT = 1 | Dynamic root (Niu et al., 2020) |

### 1.4 Model Experiments

We conducted five experiments using the current Noah-MP driven by the hourly NLDAS-2 forcing data at a spatial resolution of 0.125 degree, starting with the same uniform initial conditions—namely, soil moisture at 0.3 m3m–3 and soil temperature at 287K—spanning 2014 to 2019 for six iterations. The initial five iterations were dedicated to the model's spin-up phase, and the resulting surface and root zone soil moisture from the last iteration were used for SMM analysis. Parameters were adopted per the updates by Niu et al. (2020), with adjustments to the dynamic vegetation module to align with Moderate Resolution Imaging Spectroradiometer (MODIS) leaf area index observations. This study refrained from parameter calibration related to dual-domain schemes for preferential flow (Šimůnek & Genuchten, 2008) and ponding depth.

The five experiments are conducted with Noah-MP configurations with different water retention and infiltration schemes. Table 1 lists optional schemes that were the same for all these experiments. for other processes, including surface layer turbulent exchange, radiation transfer, phase changes between snow and rain, and the permeability of frozen soil. For this study, we selected only those schemes that have a direct impact on the simulation of soil moisture dynamics (as detailed in Table *2*). All these experiments are set with the same number of soil layers, which vary spatially from 5 – 15 vertical layers with fixed layer thicknesses: $\Delta z_i$ =0.05, 0.3, 0.6, 1.0, 2.0, 2.0, 4.0, 4.0, 5.0, 5.0, 5.0, 5.0, 5.0, 5.0, and 5.0 m down to 49.0 m to match the maximum bedrock depth data of Pelletier et al. (2016) with a minimum bedrock depth of 4.0 m. The model was customized using a combination of three soil moisture solver variants, two soil hydraulics schemes, and two ponding depth thresholds.

To explore the influence of surface ponding on SMM, we designed two distinct experimental conditions. The first condition, designated as MF_VGM0, excluded the ponding effect by setting $H_{top,max}$ to 0 mm. Conversely, the second condition, identified as MF_VGM200, incorporated a significant ponding depth of 200 mm. Both conditions utilized the mixed-form RE solver alongside the Van-Genuchten (VGM) model (refer to Table *2*). Furthermore, we conducted comparative analyses to assess the role of soil hydraulic properties by conducting experiments with the Brooks-

https://doi.org/10.5194/egusphere-2024-1256
Preprint. Discussion started: 17 May 2024


Corey/Clapp-Hornberger (BC/CH) model (MF_CH) and the VGM model (MF_VGM), each with a ponding depth threshold of $H_{top,max}$ = 50 mm.

An additional experiment employs the Dual-Permeability model (DPM) within the VGM framework, maintaining the same ponding threshold of $H_{top,max}$ = 50 mm, referred to as DPM_VGM (see Table 2). The comparison of DPM_VGM with the MF_VGM setup aimed to shed light on the effects of preferential flow channels on soil moisture forecasting, and runoff forecasting in future studies, thereby enhancing our comprehension of the complexities inherent in hydrological modeling.

To define the macropore volume fraction, we used the modeled Soil Organic Matter (SOM), which is computed from Noah-MP with a microbial-enzyme model (Zhang et al., 2014) prior to the major experiments conducted in this study through a long-term (120 years) spin-up simulation from 1980 – 2019 driven by the NLDAS data. The modeled SOM shows a pattern of more SOM in wet regions and less in arid regions due to more active microbial activities (decomposition and respiration) in wetter regions. The resulting macropore volume fraction ranges from 0.05 – 0.15 changing with spatially-varying SOM.

Table 2 Model experiment configuration.

| Experiment ID | Models | $H_{top,max}$ (mm) | Soil Hydraulics |
|---|---|---|---|
| MF_VGM0 | Mixed Form RE | 0 | Van-Genuchten |
| MF_VGM200 | Mixed Form RE | 200 | Van-Genuchten |
| MF_CH | Mixed Form RE | 50 | Brooks-Corey/Clapp-Hornberger |
| MF_VGM | Mixed Form RE | 50 | Van-Genuchten |
| DPM_VGM | DPM | 50 | Van-Genuchten |

# 2 Results

In Sections 2.1 and 2.2 of our study, we focus on computing the SMM for both the surface (5 cm) and root zone (up to 1m) layers, respectively. This dual-layer analysis is fundamental to our experiments as it allows us to understand the differential impacts of various parameterizations on soil moisture. By comparing and analyzing the SMM values across these two distinct layers, we can identify specific physical processes that influence soil moisture dynamics. This comparative approach not only elucidates how these processes affect SMM but also helps in understanding the interaction between surface characteristics and subsurface moisture dynamics, which are critical for improving hydrological modeling and prediction.

## 2.1 Long- and Short-Term Soil Moisture Memory of the Surface Layer

Figure *3* illustrates the spatial distribution of median long-term memory, derived from the five-year soil moisture dataset. Analysis of the SMAP data revealed that long-term memory ($\tau_L$) is

https://doi.org/10.5194/egusphere-2024-1256
Preprint. Discussion started: 17 May 2024


significantly higher in the energy-limited and humid regions of the eastern US, and lower in the arid western regions. These findings are consistent with those of He et al. (2023) and McColl et al. (2019).

The MF_CH experiment displays a spatial pattern that contrasts with the SMAP data, with a longer memory in the arid western regions but a shorter memory in the wet northeastern regions. Further examination reveals that models using the Van-Genuchten scheme reflect SMAP's patterns. Specifically, the eastern regions display higher $\tau_L$ values, while the western regions show lower values (see Figure 3b-f). DMP_VGM demonstrates a lower memory in the eastern CONUS compared to MF_VGM (refer to Figures 3c, d, and S1). VGM scenario with zero ponding depth shows shorter memory compared with MF_VGM200 in the eastern United States (Figures 3e and f), where surface ponding happens more frequently and with greater depth. Figure S2 shows a better match of data points with the agreement line in the DPM_VGM versus SMAP scatterplot. In contrast, the MF_CH versus SMAP scatterplot lacks this alignment, a correlation of -0.10. The correlation values have risen from –0.10 to 0.15 with VGM, a sign of progress, but they are still not strong.

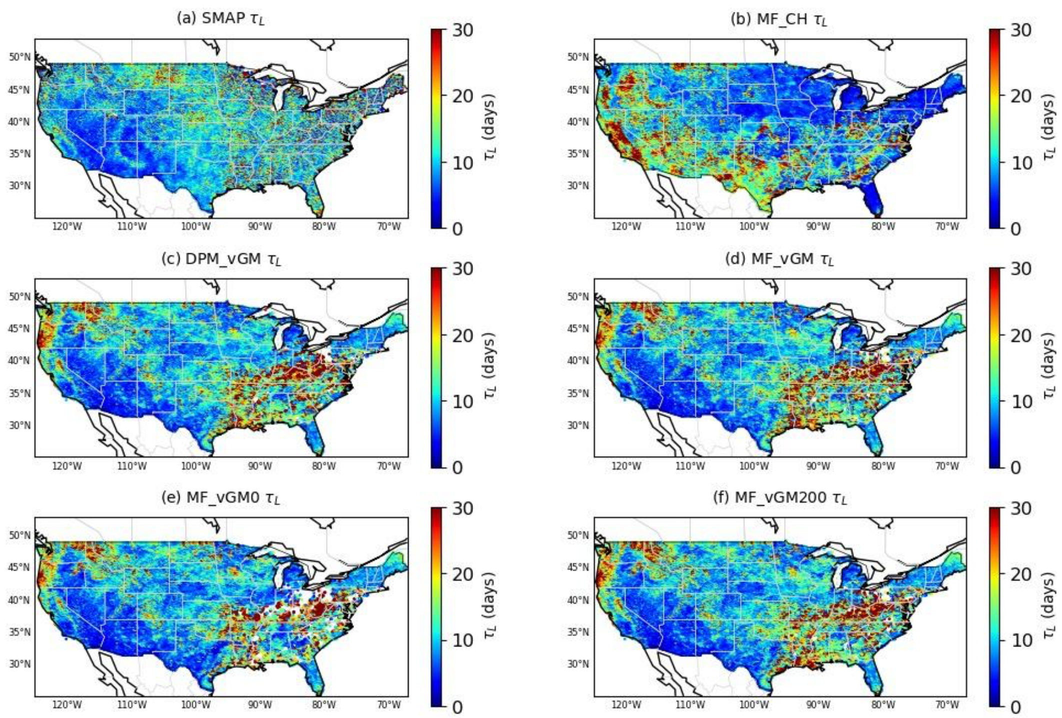


Figure 3 Long-term SMM derived from various datasets from 2015 – 2019 for soil surface layer: (a) SMAP; (b) MF_CH; (c) DMP_VGM; (d) MF_VGM; (e) MF_VGM0; and (f) MF_VGM200. SMM = Soil Moisture Memory

https://doi.org/10.5194/egusphere-2024-1256
Preprint. Discussion started: 17 May 2024


To assess the influence of plant water storage on SMAP soil moisture data and the resultant SMM, we employed the MODIS NDVI to categorize the entire CONUS into wet (NDVI > 0.45) and dry regions (NDVI < 0.45). In the dry areas (see Figure 4a), the probability distribution function (PDF) of the surface SMM from MF_CH differs from that of SMAP and exhibits a higher median of 10.53 days compared to SMAP's 8.47 days (overestimation). Other model scenarios using van Genuchten (VG) hydraulics, with an SMM median of around 8.6 days, show a distribution PDF like SMAP. Note that the VGM scenarios effectively tackle the problem of long-term memory overestimation, a point emphasized by He et al. (2023). This improvement is due to the refined parametrization of physical processes within the VGM experiments.

In the wet regions with dense vegetation (refer to Figure 4b), the SMM PDF of MF_CH (median of 8.03 days) significantly varies from SMAP PDF (median of 10.71 days), showing an underestimation of $\tau_L$. However, due to plant water storage affecting SMAP's soil moisture retrieval (commonly on eastern CONUS), our focus here is on model sensitivity to process representations rather than on model accuracy relative to SMAP data. Other models with van Genuchten (VG) scheme display greater variability among themselves in wet areas than in dry ones (Figure 4b). MF_VGM0 (with a zero ponding depth threshold) shows a decreased long-term SMM, with a median of 10.72 days, compared to MF_VGM200 (with a 200 mm threshold), with median of 12.05 days, and MF_VGM (with 50 mm ponding threshold), with a median of 12.03. Changing the ponding depth threshold from 50 mm (MF_VGM) to 200 mm (MF_vGM200), has a marginal effect on $\tau_L$, suggesting that the response does not proportionally increase with higher values. With the same 50 mm ponding threshold, DPM_VGM produces a shorter SMM, with a median of 11.73 days, than MF_VGM.

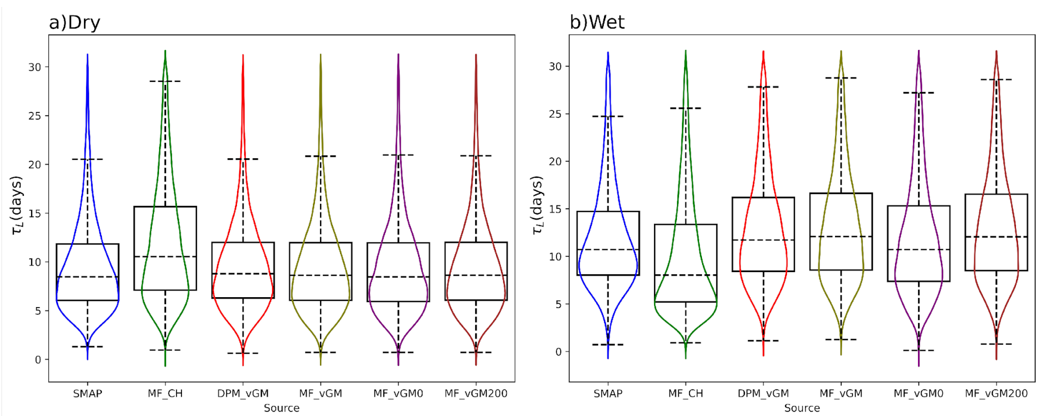


Figure 4 Violin plot of surface $\tau_L$ estimated from SMAP and Noah-MP scenarios for dry regions with less vegetation (NDVI < 0.45) and wet regions with more vegetation (NDVI > 0.45).

For the short-term SMM, all the scenarios produce an overall spatial pattern similar to that of the SMAP-derived $\tau_S$, showing a longer memory in the drier western US than in the wetter eastern (Figure 5). However, MF_CH shows a shorter memory in the northwestern US than that derived

https://doi.org/10.5194/egusphere-2024-1256
Preprint. Discussion started: 17 May 2024


from SMAP (Figure 5a & b). MF_CH with a median of 1.9 days underestimates SMAP with a median of 2.02 days, while VG scenarios have median $\tau_s$ around 2.09 days over dry regions. This effectively rectifies the underestimation in short-term memory by LSMs, as reported in previous studies (He et al., 2023). He et al. (2023) highlighted that most LSMs tend to underestimate $\tau_s$, which is strongly affected by soil water drainage as specified by McColl et al. (2019). Note that higher $\tau_s$ values indicate slow drainage, whereas lower values suggest faster drainage; this is exemplified by Figure 5a, which exposes a more rapid drainage in the eastern CONUS in contrast to the western. The incorporation of surface ponding and DPM (2.08 days) has shown less effects on short-term memory than the soil hydraulics for the dry region (more macropores are available in wet regions and hence DPM would have more effect in those regions). The introduction of surface ponding (comparing MF_VGM0 (2.11 days) to MF_VGM200 (2.108 days) in Figure 5 and Figure 6) contributes to more persistent surface soil moisture and a bit faster drainage. The pdf of SMM from all the VGM models more closely resembles the SMAP pdf in the western United States than in the eastern part of the country.

For wet regions, MF_CH with a median of 1.26 days underestimate SMAP with a median of 1.56 days. DPM_VGM with faster drainage of surface soil water produces a median $\tau_s$ of 1.43, shorter than does MF_VGM with a median of 1.48 days. The DPM model accelerates the drainage of water from the topsoil. This effect is more significant in the eastern CONUS. As a result, it lowers the short-term memory in areas where the soil has macropores.

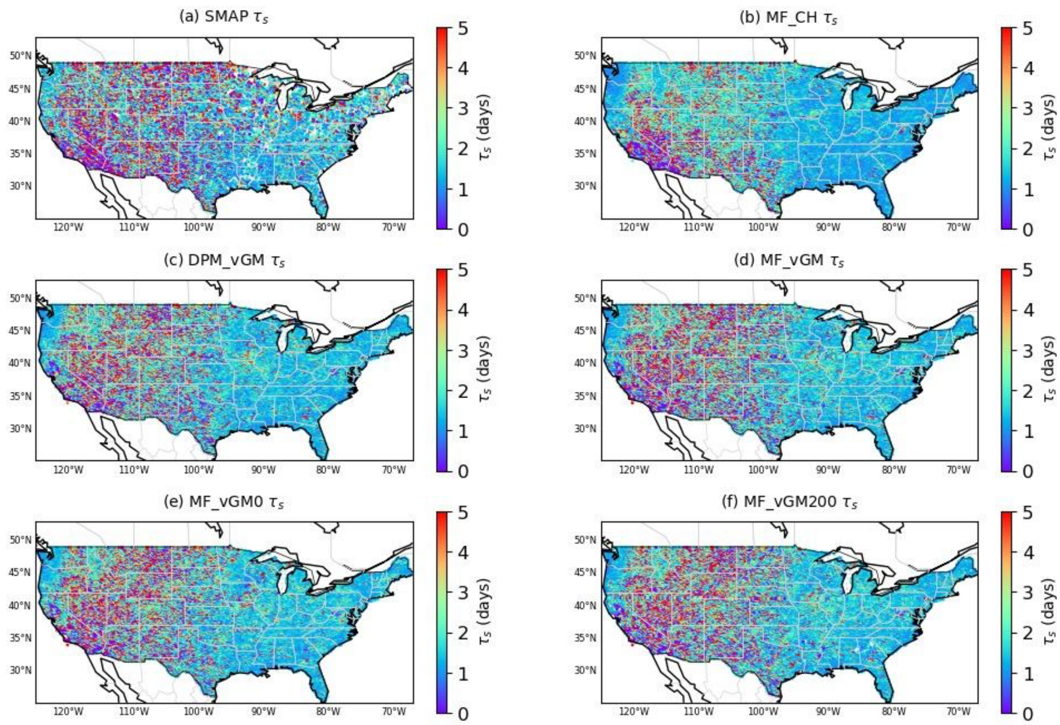


Figure 5 Short-term SMM derived from various datasets from 2015 – 2019 for soil surface layer: (a) SMAP; (b) MF_CH; (c) DMP_VGM; (d) MF_VGM; (e) MF_VGM0; and (f)

https://doi.org/10.5194/egusphere-2024-1256
Preprint. Discussion started: 17 May 2024


MF_VGM200. SMM = Soil Moisture Memory.

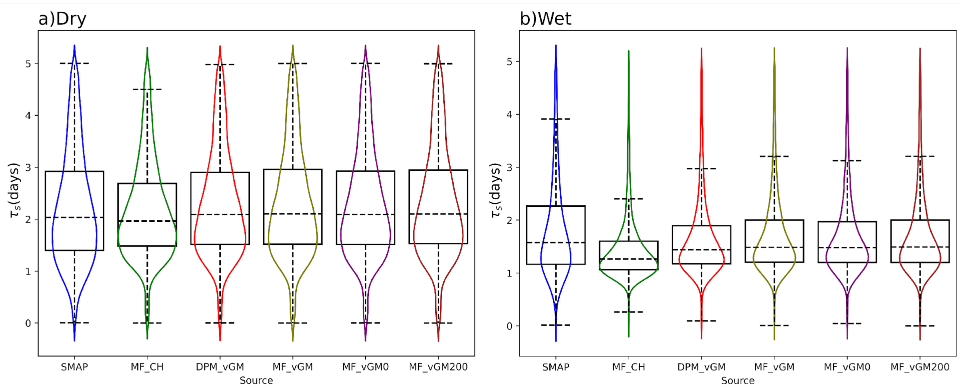


Figure 6 Same as Figure 4 for short-term memory.

## 2.2 Long- and Short-Term Soil Moisture Memory of the Root Zone Layers

We use the International Soil Moisture Network (ISMN) soil moisture dataset as the benchmark and compute SMM at the ISMN stations as illustrated in Figure 2. We compute the long-term SMM across 654 sites within CONUS for the period from 2015 – 2019. The median values of these computations indicate that the root zone SMM (Figure 7 & Figure 9) is generally higher than the surface SMM (Figure 3 & Figure 5). Analysis of ISMN data reveals that the root zone $\tau_L$ (Figure 7) generally exceeds surface $\tau_L$ (Figure 3), particularly longer in the western US. Some eastern locations also exhibit longer $\tau_L$, whereas the central region demonstrates lower values.

MF_CH produces a shorter root-zone $\tau_L$ across nearly all the sites in CONUS (Figure 7 & Figure *8*). The Van-Genuchten scheme mirrors the ISMN-derived $\tau_L$, albeit with slightly higher values (Figure 7 & Figure 8). An increase in surface ponding depth raises the $\tau_L$. This is particularly true in the eastern US, where surface ponding occurs more often, and its impact on soil moisture is more substantial. Figures S3 and S4 illustrate this effect. Additionally, DMP_VGM (Figure 7c and Figure 8) reduces the root-zone long-term SMM across most of CONUS relative to the other models (Figure 7c, d, e, & f and Figure S3).

https://doi.org/10.5194/egusphere-2024-1256
Preprint. Discussion started: 17 May 2024


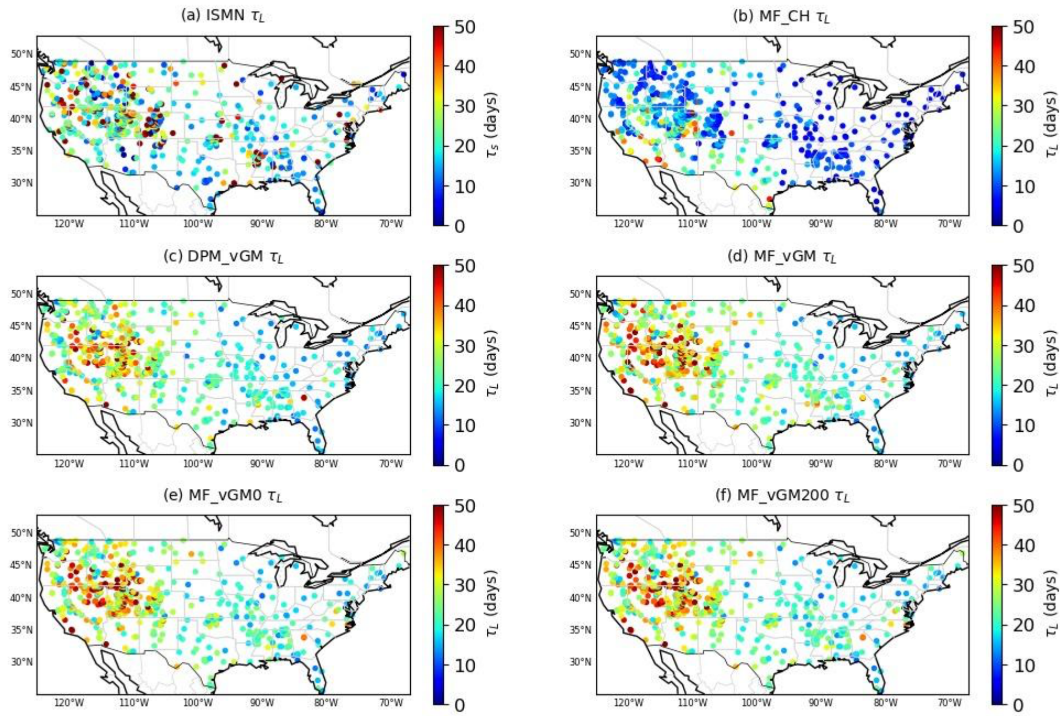


Figure 7 Long-term root-zone SMM derived from various datasets from 2015 – 2019: (a) ISMN; (b) MF_CH; (c) DMP_VGM; (d) MF_VGM; (e) MF_VGM0; and (f) MF_VGM200. SMM = Soil Moisture Memory.

553
554

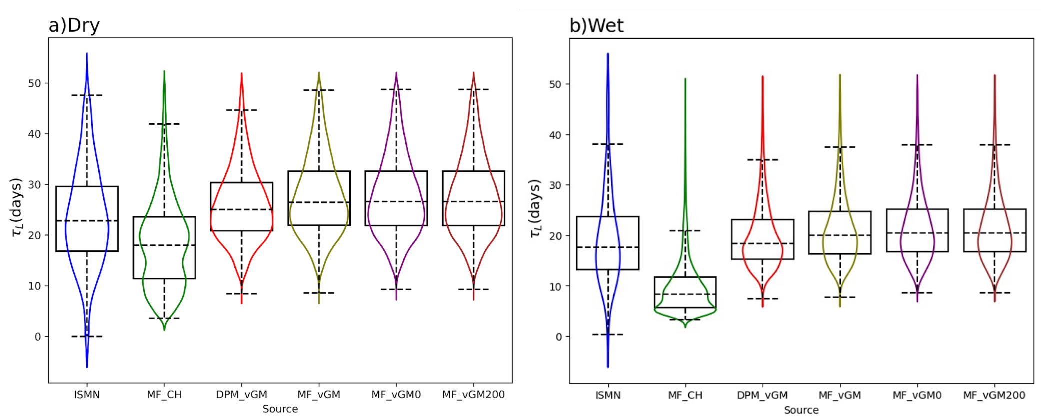


Figure 8 Violin plot of root zone $\tau_L$ estimated from ISMN and Noah-MP scenarios for dry regions with less vegetation (NDVI < 0.45) and wet regions with more vegetation (NDVI > 0.45).

https://doi.org/10.5194/egusphere-2024-1256
Preprint. Discussion started: 17 May 2024


As for the surface layer, we use the MODIS NDVI to classify all the stations into wet and dry regions. In the dry regions (Figure 8a), MF_CH has a different probability distribution function and a lower median of 19 days compared to that of ISMN (median of 23 days). All the other scenarios using VG schemes exhibit a similar SMM PDF to each other, yet they are somewhat different from the one derived from ISMN. Also, the presence of macropores reduces long-term SMM, with a median of 25 days, and results in the closest median to the ISMN (Figure 8a). ISMN, however, shows a large range of long-term SMM compared with all the Noah-MP experiments, indicating the complex nature of the observed SMM needs further investigation (Figure 8a & b). Note that the analyses were conducted at a limited number of locations, presenting challenges in fully capturing the impacts of different parameterizations on SMM.

In the wet regions, MF_CH shows smaller $\tau_L$ values (median of 9.8 days) than that from ISMN (median of 18 days) together with a noticeable pdf difference. The effect of dual permeability decreases the soil moisture and long-term memory compared with the other model experiments, resulting in a median (19 days) close to ISMN (18 days), Figure 8b. However, it seems that the ponding depth does not show a noticeable impact on $\tau_L$. It should be noted that the effect of ponding depth, which slightly increases the long-term memory in RTZ, can be observed in Figure S3 and Figure S4 when we take a close look into them.

Further investigation reveals an enhancement in the model's ability to capture soil hydraulic dynamics when shifting from the Clapp-Hornberger to the Van-Genuchten scheme, with an improvement in $\tau_L$values from 0.05 to 0.12 (Figure S5). Also, The Dual Permeability model with Van-Genuchten (DPM_VGM) demonstrates superior performance with a correlation of 0.15, compared to all other scenarios tested.

https://doi.org/10.5194/egusphere-2024-1256
Preprint. Discussion started: 17 May 2024


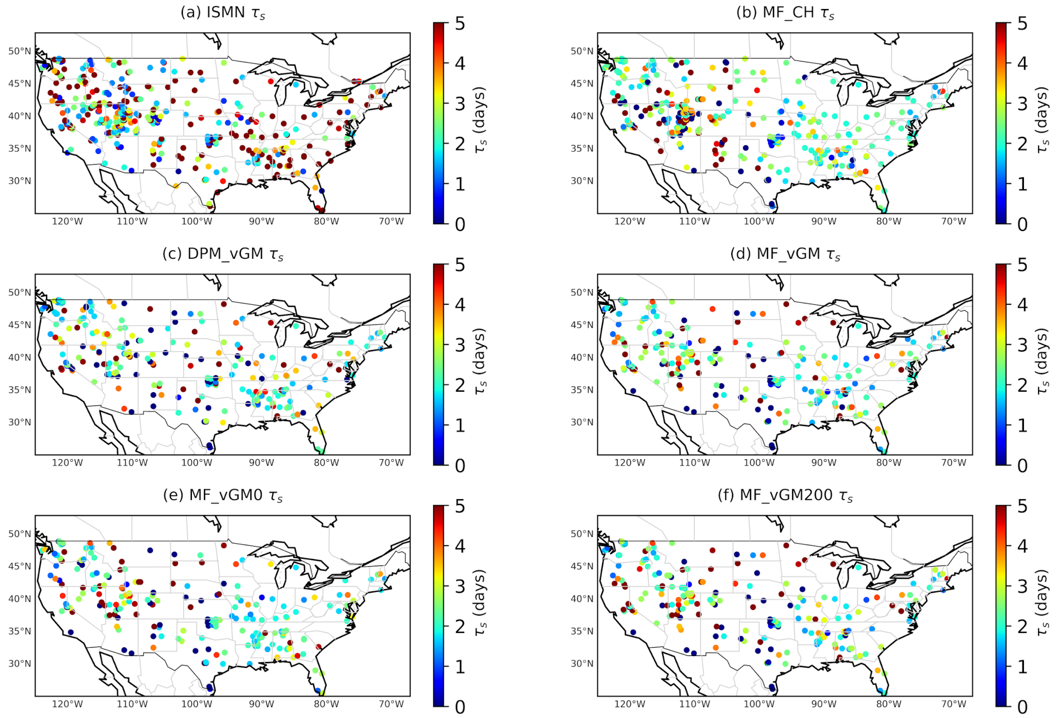


Figure 9 Same as Figure 7 but for short-term.

The findings show that $\tau_s$ in most Noah-MP scenarios are comparable to those observed in the ISMN data, as shown in Figure 9b to f. However, there is a consistent underestimation in some eastern locations. Figure 10 highlights this pattern, showing that wet regions tend to underestimate $\tau_s$, with ISMN reporting a median of 2.5 days and Noah-MP experiments a median of around 2 days. Conversely, dry regions tend to overestimate, with ISMN at a median of 2.1 days and Noah-MP experiments at approximately 2.7 days.

Although distinguishing between MF_VGM0 and MF_VGM200 in Figure 9 and Figure 10 is challenging, Figure 11 (Figure 11c and d) reveals that an increase in ponding depth leads to a slight decrease in short-term memory in the eastern CONUS. Comparing Figure 9 with Figure 11 indicates that ISMN stations partially reflect the spatial pattern of long-term and short-term memory in the root zone across CONUS. It may be concluded that the spatial patterns of long-term and short-term memory (Figure 11 and Figure S7) of the root zone are quite similar to those of the surface layer (Figure 3 and Figure 5). Hence, long-term memory is more prevalent in the eastern CONUS and mountainous areas, while longer short-term memory occurs predominantly in western areas. However, this conclusion is not totally true and further investigation is needed.

https://doi.org/10.5194/egusphere-2024-1256
Preprint. Discussion started: 17 May 2024


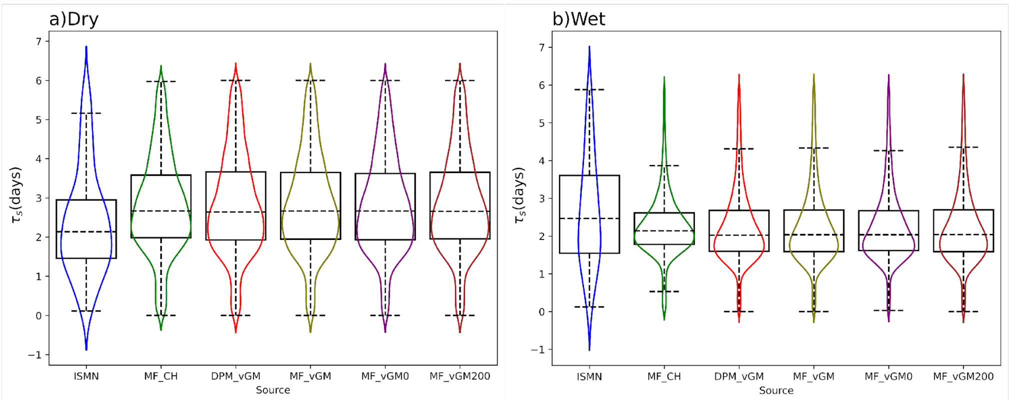


Figure 10 Same as Figure 8 but for short-term.

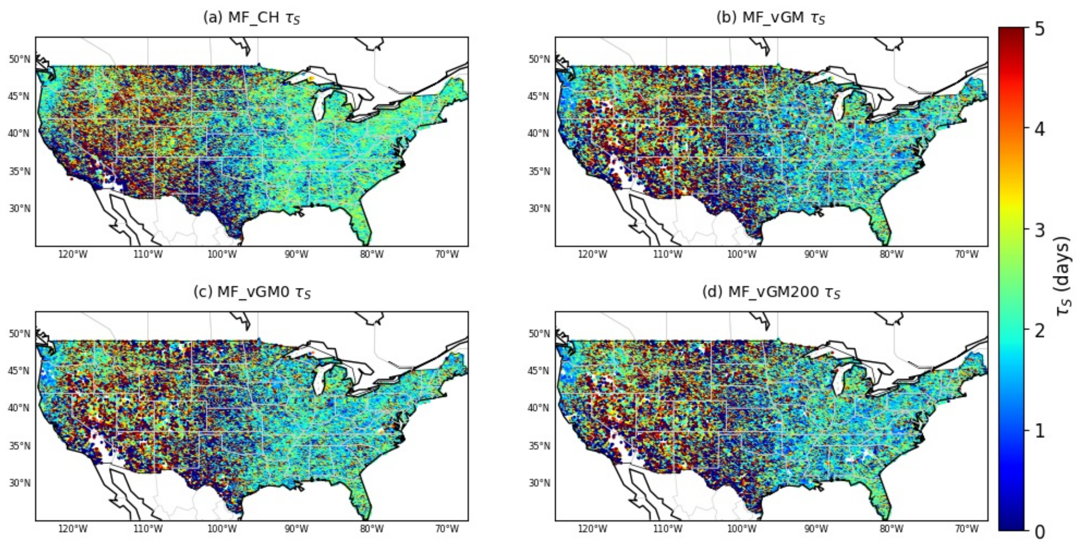


Figure 11 Spatial distribution of root zone $\tau_s$ estimated from (a) MF_CH; (b) MF_VGM; (c) MF_VGM0; and (d) MF_VGM0.

# 3 Discussion

## 3.1 How Do Different Parametrizations Affect SMM?

The efficacy of LSMs in simulating climate feedback mechanisms critically depends on the soil's ability to retain moisture and how fast the soil releases the moisture up to the atmosphere through soil surface evaporation and plant transpiration and down to the aquifers through recharge. The rapid infiltration of incident water (rainfall and snowmelt) into deeper subsoil strata reduces the soil's capacity to return moisture to the atmosphere through evaporation and transpiration. Thereby

https://doi.org/10.5194/egusphere-2024-1256
Preprint. Discussion started: 17 May 2024


disrupting potential atmospheric feedback loops in LSMs (Mccoll et al., 2019). Conversely, If LSMs lose water too quickly through evapotranspiration, they provide feedback to the atmosphere faster than they should. Thus, the concept of SMM becomes essential in LSMs, as it can provide information about the rate at which moisture disappears from soil. Hence, understanding the effects of various physical processes on SMM is vital for enhancing the representation of these processes in LSMs, thereby improving their overall performance in simulating the complex interactions between the land surface and the atmosphere.

The water retention curve characteristics of the BC/CH hydraulics scheme are characterized by a strong suction force that is more pronounced than in the Van-Genuchten model for various soil types (Niu et al, 2024). This stronger suction promotes moisture transfer from the deeper layers to the surface layer, causing the surface soil to retain more moisture (Figure S6) and has a longer $\tau_L$(Figure 3, 4), a common issue in LSMs according to He et al. (2023). Moreover, the higher suction reduces the root zone moisture and consequently, it would have a shorter $\tau_L$(Figure 7, 8). Conversely, the VG scheme, with weaker suction, transfers less moisture from the root zone to the surface, resulting in a drier surface layer and a shorter $\tau_L$ for the surface, but a longer $\tau_L$ for the root zone, as depicted in Figures 7 and 8.

Short-term memory is inversely related to moisture availability; thus, the more wet soil has the shorter $\tau_S$, while a drier layer has a longer $\tau_S$. The VG scheme produces a drier surface layer and a moister root zone, leading to a longer surface $\tau_S$ and a shorter root zone $\tau_S$ compared to the BC scheme, shown in Figures 5, 6, and 11.

As indicated in a previous study by He et al. (2023), a common issue in LSMs is the overestimation of the long-term memory of surface soil over dry regions. This could be because of an underestimation of evaporation within LSMs using CH parametrization (Figure S7a), resulting in overestimation of soil moisture. However, a shift towards the Van-Genuchten (VG) parametrization increases the evaporation (Figure S7b, Figure S8), and hence it overcomes the $\tau_L$ overestimation (Figure 3, 4).

The presence of soil macropores promotes infiltration at the soil surface and preferential flow from the surface to the root zone (Mohammed et al., 2021), consequently reducing the moisture retained in the surface layer. Moreover, macropores lead to reduced suction of the soil, hence less water from subsurface soil was pulled up to the surface, causing the topsoil to have less moisture (Figure S6). Therefore, macropores lead to a decrease of surface $\tau_L$(Figure 3d, 4b). Moreover, the presence of macropores increases root zone soil moisture and consequently, it should prolong the root zone $\tau_L$. However, the even distribution of macropores throughout the soil profile in current Noah-MP configuration, DPM_VGM, increases water infiltration into deeper layers, resulting in faster recharge of the deep soil and drier root zone. As a result, macropores reduce the root-zone long-term SMM (Figure 7d, e, & f and Figure S8) of DPM_VGM. This highlights the importance of calibration of macropore profile in DPM_VGM for better representation of macropores and soil hydrohalic dynamics.

While the soil matrix typically allows for only slow water movement due to the pressure gradient, macropores enable rapid gravitational flow (Mohammed et al., 2018). These macropores facilitate quicker infiltration to the root zone (Mohammed et al., 2021). Therefore, they increase the drainage

https://doi.org/10.5194/egusphere-2024-1256
Preprint. Discussion started: 17 May 2024


rate to these deeper layers, which consequently slightly reduces the short-term soil moisture memory in the surface (Figures 5, 6). Additionally, as water moves from the surface to the root zone, the increased moisture content there leads to quicker drainage (we speculate that this occurs in the real world; however, in the current DPM_VGM, the deep soil is wetter than root zone, indicating a need for calibration of the macropore profile as we have stated). Consequently, this process further decreases the short-term moisture memory in the root zone due to the higher drainage rates of wetter soil.

Finally, the ponding threshold allows water to remain on the surface before turning into runoff. This provides water with more time to percolate into the soil. The consequent increase in ponding depth allows extended water infiltration, thus enhancing soil moisture and lengthening moisture retention through the soil profile (Figure S6e, f). So as discussed before, wetter soil leads to prolong $\tau_L$ and shorten $\tau_S$ (Figure 5, 6, 7, 11).

### 3.2 Limitation of Our Study

Some sources of uncertainty may affect our results in this study, including uncertainties in input data, and models. SMAP reliability is affected by plant water storage change (in the eastern part and some mountainous sites), introducing uncertainties into SMM values for the benchmark. While the SMAP observation over some eastern parts and mountainous areas may not be reliable (e.g., due to dense vegetation), it still serves our objective of deepening our understanding of the physical process involved in soil hydrohalic/hydrology. Furthermore, the SMM patterns captured from SMAP can be insightful in understanding regional variabilities in SMM.

Another concern is the influence of ISMN spatial representation on SMM analysis. ISMN stations are point-based, and it is assumed that one point represents a 1/8-degree grid area. It is possible that the point measurements cannot be representative of the Noah-MP spatial grids. Therefore, discrepancies in capturing values or spatial patterns might be attributed to the scale difference between point and grid data. Additionally, the limited number of stations could be a contributing factor.

Additionally, certain model assumptions may require further investigation. The DPM_VGM scheme uses vertically constant macropore volume fraction, which means macropores generated due to wormhole and tree roots are fixed down to the bedrock. However, in nature, these macropores would reduce after a few meters from the soil top. Because the existence of macropores in nature drains the surface layer and increases the root zone soil moisture, to better represent the actual physical process, it is necessary to calibrate macropore volume fraction within Noah-MP. Such calibration is anticipated to further advance the fidelity of soil moisture simulations, enhancing the model's utility in various hydrological and climatological applications.

Concerning surface water ponding, a constant ponding threshold may not be justified, and a spatially variable surface ponding may lead to improved model accuracy. We expect calibration of this parameter to achieve a more realistic representation of the soil hydraulic process.

There are additional factors, such as lateral flow, that may affect SMM but were not considered in our analysis. The primary focus of our study was to understand the underlying processes in SMM

https://doi.org/10.5194/egusphere-2024-1256
Preprint. Discussion started: 17 May 2024


and utilize this understanding to guide the selection of parameterizations in the Noah-MP model. Consequently, we narrowed our examination to those parameters and processes represented within Noah-MP. Future research could further evaluate the impact of lateral flow and other processes on SMM, expanding our understanding of these dynamics and their implications for land surface modeling.

## 4 Conclusion

In this study, we have explored the effects of soil hydraulic parameterizations on SMM using the Noah-MP land surface model. Our research was driven by a desire to understand the physical processes that influence SMM and to address the commonly observed overestimation/underestimation of long-term/short-term SMM in LSMs. With these insights, we aimed to improve the representation of soil hydrology within Noah-MP, utilizing the knowledge gained from our analysis of SMM. We designed and implemented five scenarios to assess the impacts of different parametrizations. These scenarios include two soil hydraulic models (Clapp and Hornberger and Van-Genuchten), a dual permeability infiltration scheme, and three variations of surface ponding depth. Utilizing soil moisture datasets from SMAP and ISMN for surface and root zone measurements, respectively, we conducted a comprehensive analysis of the effects of different Noah-MP parameterizations on soil moisture memory.

Our findings demonstrate that the soil retention curve has an important effect on SMM, due to its influence on the existing suction in the soil. We have demonstrated that the adoption of the Van-Genuchten (VG) parameterization considerably mitigates the long-standing issue of overestimating SMM in LSMs employing Brooks-Corey/Clapp-Hornberger (BC/CH) models. The Van-Genuchten model, with its reduced suction effect attributable to a drier surface layer, leads to a more accurate depiction of moisture transfer from the root zone to the surface, which is important for realistic soil moisture dynamics.

Moreover, incorporating surface ponding allows for extended soil water infiltration, thus refining both surface and root zone moisture conditions. This leads to an increase in long-term memory and a decrease in short-term memory. The inclusion of a dual permeability approach fine-tunes soil moisture representation by accounting for preferential flow paths, marking a step forward in the enhancement of soil moisture memory and the overall fidelity of hydrological simulations. Macropores lead to a decrease in short-term memory due to their effects on the enhancement of drainage. Furthermore, macropores lead to a decrease in long-term memory, due to its effects on draining and decreasing surface soil moisture. Nevertheless, our analyses underscore the necessity for calibration of the macropore fraction and ponding depth to further refine the soil hydraulic dynamics within the Noah-MP model. Given these compelling advancements, it is our strong recommendation that LSMs adopt VG hydraulics to advance the prediction of hydrological and climatic phenomena.

## Competing interests

The contact author has declared that none of the authors has any competing interests.

## Acknowledgments

Funding for this project was provided by the National Oceanic and Atmospheric Administration (NOAA), awarded to the Cooperative Institute for Research on Hydrology (CIROH) through the NOAA Cooperative Agreement with The University of Alabama, NA22NWS4320003. Also, the research carried out for this article was supported by the U.S. Army Corps of Engineers, Engineer Research and Development Center, Coastal Inlets Research Program via Congressionally Directed R&D with the National Oceanic and Atmospheric Administration's National Water Center. The data used in this study are freely available online:
NLDAS-2 data (http://www.emc.ncep.noaa.gov/mmb/nldas/); NASA SMAP soil moisture product (https://nsidc.org/data/spl3smp_e/versions/6); GPM IMERG-Final product (https://disc.gsfc.nasa.gov/datasets/GPM_3IMERGHH_06/summary). The Noah-MP code used in this study has been uploaded to a repository that may be accessed by other researchers (https://github.com/mfarmani95/NoahMP_Dual).

## Reference

A. Boone. (2004). *The Rhône-Aggregation Land Surface Scheme intercomparison project: An overview.* (Vol. 17, pp. 187–208). https://doi.org/https://doi.org/10.1175/1520-0442(2004)017<0187:TRLSSI>2.0.CO;2
Agnihotri, J., Behrangi, A., Tavakoly, A., Geheran, M., Farmani, M. A., & Niu, G. Y. (2023). Higher Frozen Soil Permeability Represented in a Hydrological Model Improves Spring Streamflow Prediction From River Basin to Continental Scales. *Water Resources Research*, *59*(4). https://doi.org/10.1029/2022WR033075
Chen, F., & Dudhia, J. (2001). Coupling an Advanced Land Surface–Hydrology Model with the Penn State–NCAR MM5 Modeling System. Part I: Model Implementation and Sensitivity. *Monthly Weather Review*, *129*(4), 569–585. https://doi.org/10.1175/1520-0493(2001)129<0569:CAALSH>2.0.CO;2
Colliander, A., Jackson, T. J., Bindlish, R., Chan, S., Das, N., Kim, S. B., Cosh, M. H., Dunbar, R. S., Dang, L., Pashaian, L., Asanuma, J., Aida, K., Berg, A., Rowlandson, T., Bosch, D., Caldwell, T., Caylor, K., Goodrich, D., al Jassar, H., … Yueh, S. (2017). Validation of SMAP surface soil moisture products with core validation sites. *Remote Sensing of Environment*, *191*, 215–231. https://doi.org/10.1016/j.rse.2017.01.021
Delworth, T. L., & Manabe, S. (1988). The Influence of Potential Evaporation on the Variabilities of Simulated Soil Wetness and Climate. *Journal of Climate*, *1*(5), 523–547. https://doi.org/10.1175/1520-0442(1988)001<0523:TIOPEO>2.0.CO;2
Delworth, T., & Manabe, S. (1989). The Influence of Soil Wetness on Near-Surface Atmospheric Variability. *Journal of Climate*, *2*(12), 1447–1462. https://doi.org/10.1175/1520-0442(1989)002<1447:TIOSWO>2.0.CO;2
Dirmeyer, P. A. (2011). The terrestrial segment of soil moisture-climate coupling. *Geophysical Research Letters*, *38*(16), n/a-n/a. https://doi.org/10.1029/2011GL048268
Dorigo, W. A., Wagner, W., Hohensinn, R., Hahn, S., Paulik, C., Xaver, A., Gruber, A., Drusch, M., Mecklenburg, S., van Oevelen, P., Robock, A., & Jackson, T. (2011). The International Soil Moisture Network: a data hosting facility for global in situ soil moisture measurements. *Hydrology and Earth System Sciences*, *15*(5), 1675–1698. https://doi.org/10.5194/hess-15-1675-2011
Entekhabi, D., Njoku, E. G., O'Neill, P. E., Kellogg, K. H., Crow, W. T., Edelstein, W. N., Entin, J. K., Goodman, S. D., Jackson, T. J., Johnson, J., Kimball, J., Piepmeier, J. R., Koster, R. D., Martin, N., McDonald, K. C., Moghaddam, M., Moran, S., Reichle, R., Shi, J. C., … Van Zyl, J. (2010). The Soil Moisture Active Passive (SMAP) Mission. *Proceedings of the IEEE*, *98*(5), 704–716. https://doi.org/10.1109/JPROC.2010.2043918
Findell, K. L., Gentine, P., Lintner, B. R., & Kerr, C. (2011). Probability of afternoon precipitation in eastern United States and Mexico enhanced by high evaporation. *Nature Geoscience*, *4*(7), 434–439. https://doi.org/10.1038/ngeo1174

https://doi.org/10.5194/egusphere-2024-1256
Preprint. Discussion started: 17 May 2024


Ghannam, K., Nakai, T., Paschalis, A., Oishi, C. A., Kotani, A., Igarashi, Y., Kumagai, T., & Katul, G. G. (2016). Persistence and memory timescales in root-zone soil moisture dynamics. *Water Resources Research*, *52*(2), 1427–1445. https://doi.org/10.1002/2015WR017983

Guo, Z., Dirmeyer, P. A., Hu, Z.-Z., Gao, X., & Zhao, M. (2006). Evaluation of the Second Global Soil Wetness Project soil moisture simulations: 2. Sensitivity to external meteorological forcing. *Journal of Geophysical Research: Atmospheres*, *111*(D22). https://doi.org/10.1029/2006JD007845

He, Q., Lu, H., & Yang, K. (2023). Soil Moisture Memory of Land Surface Models Utilized in Major Reanalyses Differ Significantly From SMAP Observation. *Earth's Future*, *11*(4). https://doi.org/10.1029/2022EF003215

Huffman, G. J., Bolvin, D. T., Braithwaite, D., Hsu, K. L., Joyce, R. J., Kidd, C., Nelkin, E. J., Sorooshian, S., Stocker, E. F., Tan, J., Wolff, D. B., & Xie, P. (2020). Integrated Multi-satellite Retrievals for the Global Precipitation Measurement (GPM) Mission (IMERG). *Advances in Global Change Research*, *67*, 343–353. https://doi.org/10.1007/978-3-030-24568-9_19/FIGURES/3

Katul, G. G., Porporato, A., Daly, E., Oishi, A. C., Kim, H., Stoy, P. C., Juang, J., & Siqueira, M. B. (2007). On the spectrum of soil moisture from hourly to interannual scales. *Water Resources Research*, *43*(5). https://doi.org/10.1029/2006WR005356

Koster, R. D., Dirmeyer, P. A., Guo, Z., Bonan, G., Chan, E., Cox, P., Gordon, C. T., Kanae, S., Kowalczyk, E., Lawrence, D., Liu, P., Lu, C. H., Malyshev, S., McAvaney, B., Mitchell, K., Mocko, D., Oki, T., Oleson, K., Pitman, A., … Yamada, T. (2004). Regions of strong coupling between soil moisture and precipitation. *Science*, *305*(5687), 1138–1140. https://doi.org/10.1126/SCIENCE.1100217/ASSET/7E646D5F-3673-4662-893C-3764097B2395/ASSETS/GRAPHIC/ZSE0320427700002.JPEG

Koster, R. D., Dirmeyer, P. A., Hahmann, A. N., Ijpelaar, R., Tyahla, L., Cox, P., & Suarez, M. J. (2002). *Comparing the Degree of Land-Atmosphere Interaction in Four Atmospheric General Circulation Models*.

Koster, R. D., Guo, Z., Yang, R., Dirmeyer, P. A., Mitchell, K., & Puma, M. J. (2009). On the Nature of Soil Moisture in Land Surface Models. *Journal of Climate*, *22*(16), 4322–4335. https://doi.org/10.1175/2009JCLI2832.1

Koster, R. D., & Mahanama, S. P. P. (2012). Land surface controls on hydroclimatic means and variability. *Journal of Hydrometeorology*, *13*(5), 1604–1620. https://doi.org/10.1175/JHM-D-12-050.1

Koster, R. D., Mahanama, S. P. P., Livneh, B., Lettenmaier, D. P., & Reichle, R. H. (2010). Skill in streamflow forecasts derived from large-scale estimates of soil moisture and snow. *Nature Geoscience*, *3*(9), 613–616. https://doi.org/10.1038/ngeo944

Koster, R. D., Reichle, R. H., & Mahanama, S. P. P. (2017). A Data-Driven Approach for Daily Real-Time Estimates and Forecasts of Near-Surface Soil Moisture. *Journal of Hydrometeorology*, *18*(3), 837–843. https://doi.org/10.1175/JHM-D-16-0285.1

Koster, R. D., Schubert, S. D., & Suarez, M. J. (2009a). Analyzing the Concurrence of Meteorological Droughts and Warm Periods, with Implications for the Determination of Evaporative Regime. *Journal of Climate*, *22*(12), 3331–3341. https://doi.org/10.1175/2008JCLI2718.1

Koster, R. D., Schubert, S. D., & Suarez, M. J. (2009b). Analyzing the Concurrence of Meteorological Droughts and Warm Periods, with Implications for the Determination of Evaporative Regime. *Journal of Climate*, *22*(12), 3331–3341. https://doi.org/10.1175/2008JCLI2718.1

Koster, R. D., & Suarez, M. J. (1999). *A Simple Framework for Examining the Interannual Variability of Land Surface Moisture Fluxes*.

Koster, R. D., & Suarez, M. J. (2001). Soil Moisture Memory in Climate Models. *Journal of Hydrometeorology*, *2*(6), 558–570. https://doi.org/10.1175/1525-7541(2001)002<0558:SMMICM>2.0.CO;2

Mao, Y., Crow, W. T., & Nijssen, B. (2020). A Unified Data-Driven Method to Derive Hydrologic Dynamics From Global SMAP Surface Soil Moisture and GPM Precipitation Data. *Water Resources Research*, *56*(2). https://doi.org/10.1029/2019WR024949

McColl, K. A., Alemohammad, S. H., Akbar, R., Konings, A. G., Yueh, S., & Entekhabi, D. (2017). The global distribution and dynamics of surface soil moisture. *Nature Geoscience*, *10*(2), 100–104. https://doi.org/10.1038/ngeo2868

Mccoll, K. A., He, Q., Lu, H., & Entekhabi, D. (2019). Short-term and long-term surface soil moisture memory time scales are spatially anticorrelated at global scales. *Journal of Hydrometeorology*, *20*(6), 1165–1182. https://doi.org/10.1175/JHM-D-18-0141.1

McColl, K. A., Wang, W., Peng, B., Akbar, R., Short Gianotti, D. J., Lu, H., Pan, M., & Entekhabi, D. (2017a). Global characterization of surface soil moisture drydowns. *Geophysical Research Letters*, *44*(8), 3682–3690. https://doi.org/10.1002/2017GL072819

https://doi.org/10.5194/egusphere-2024-1256
Preprint. Discussion started: 17 May 2024


McColl, K. A., Wang, W., Peng, B., Akbar, R., Short Gianotti, D. J., Lu, H., Pan, M., & Entekhabi, D. (2017b). Global characterization of surface soil moisture drydowns. *Geophysical Research Letters*, *44*(8), 3682–3690. https://doi.org/10.1002/2017GL072819

Mei, R., & Wang, G. (2012). Summer Land–Atmosphere Coupling Strength in the United States: Comparison among Observations, Reanalysis Data, and Numerical Models. *Journal of Hydrometeorology*, *13*(3), 1010–1022. https://doi.org/10.1175/JHM-D-11-075.1

Moghisi, S. S., Yazdi, J., & Salehi Neyshabouri, S. A. A. (2024). Multivariate Analysis of Rainfall Spatial Distribution and Its Effect on Stormwater Magnitudes. *Journal of Hydrologic Engineering*, *29*(2). https://doi.org/10.1061/JHYEFF.HEENG-5941

Nakai, T., Katul, G. G., Kotani, A., Igarashi, Y., Ohta, T., Suzuki, M., & Kumagai, T. (2014). Radiative and precipitation controls on root zone soil moisture spectra. *Geophysical Research Letters*, *41*(21), 7546–7554. https://doi.org/10.1002/2014GL061745

Niu, G., Fang, Y., Chang, L., Jin, J., Yuan, H., & Zeng, X. (2020). Enhancing the Noah-MP Ecosystem Response to Droughts With an Explicit Representation of Plant Water Storage Supplied by Dynamic Root Water Uptake. *Journal of Advances in Modeling Earth Systems*, *12*(11). https://doi.org/10.1029/2020MS002062

Niu, G. Y., Yang, Z. L., Mitchell, K. E., Chen, F., Ek, M. B., Barlage, M., Kumar, A., Manning, K., Niyogi, D., Rosero, E., Tewari, M., & Xia, Y. (2011). The community Noah land surface model with multiparameterization options (Noah-MP): 1. Model description and evaluation with local-scale measurements. *Journal of Geophysical Research Atmospheres*, *116*(12). https://doi.org/10.1029/2010JD015139

Oleson, K. W., Lawrence, D. M., Bonan, G. B., Flanner, M. G., Kluzek, E., Lawrence, P. J., Levis, S., Swenson, S. C., Thornton, P. E., Dai, A., Decker, M., Dickinson, R., Feddema, J., Heald, C. L., Hoffman, F., Lamarque, J.-F., Mahowald, N., Niu, G.-Y., Qian, T., … Zeng, X. (2010). *Technical Description of version 4.0 of the Community Land Model (CLM)*. https://doi.org/10.5065/D6FB50WZ

Pastorello, G., Trotta, C., Canfora, E., Chu, H., Christianson, D., Cheah, Y. W., Poindexter, C., Chen, J., Elbashandy, A., Humphrey, M., Isaac, P., Polidori, D., Ribeca, A., van Ingen, C., Zhang, L., Amiro, B., Ammann, C., Arain, M. A., Ardö, J., … Papale, D. (2020). The FLUXNET2015 dataset and the ONEFlux processing pipeline for eddy covariance data. *Scientific Data 2020 7:1*, *7*(1), 1–27. https://doi.org/10.1038/s41597-020-0534-3

Pelletier, J. D., Broxton, P. D., Hazenberg, P., Zeng, X., Troch, P. A., Niu, G., Williams, Z., Brunke, M. A., & Gochis, D. (2016). A gridded global data set of soil, intact regolith, and sedimentary deposit thicknesses for regional and global land surface modeling. *Journal of Advances in Modeling Earth Systems*, *8*(1), 41–65. https://doi.org/10.1002/2015MS000526

Seneviratne, S. I., & Koster, R. D. (2012). A Revised Framework for Analyzing Soil Moisture Memory in Climate Data: Derivation and Interpretation. *Journal of Hydrometeorology*, *13*(1), 404–412. https://doi.org/10.1175/JHM-D-11-044.1

Seneviratne, S. I., Koster, R. D., Guo, Z., Dirmeyer, P. A., Kowalczyk, E., Lawrence, D., Liu, P., Mocko, D., Lu, C.-H., Oleson, K. W., & Verseghy, D. (2006). Soil Moisture Memory in AGCM Simulations: Analysis of Global Land–Atmosphere Coupling Experiment (GLACE) Data. *Journal of Hydrometeorology*, *7*(5), 1090–1112. https://doi.org/10.1175/JHM533.1

Seneviratne, S. I., Lüthi, D., Litschi, M., & Schär, C. (2006). Land–atmosphere coupling and climate change in Europe. *Nature 2006 443:7108*, *443*(7108), 205–209. https://doi.org/10.1038/nature05095

Shellito, P. J., Small, E. E., Colliander, A., Bindlish, R., Cosh, M. H., Berg, A. A., Bosch, D. D., Caldwell, T. G., Goodrich, D. C., McNairn, H., Prueger, J. H., Starks, P. J., van der Velde, R., & Walker, J. P. (2016). SMAP soil moisture drying more rapid than observed in situ following rainfall events. *Geophysical Research Letters*, *43*(15), 8068–8075. https://doi.org/10.1002/2016GL069946

Shellito, P. J., Small, E. E., & Livneh, B. (2018). Controls on surface soil drying rates observed by SMAP and simulated by the Noah land surface model. *Hydrology and Earth System Sciences*, *22*(3), 1649–1663. https://doi.org/10.5194/hess-22-1649-2018

Šimůnek, J., & Genuchten, M. Th. (2008). Modeling Nonequilibrium Flow and Transport Processes Using HYDRUS. *Vadose Zone Journal*, *7*(2), 782–797. https://doi.org/10.2136/vzj2007.0074

Taylor, C. M., de Jeu, R. A. M., Guichard, F., Harris, P. P., & Dorigo, W. A. (2012). Afternoon rain more likely over drier soils. *Nature*, *489*(7416), 423–426. https://doi.org/10.1038/nature11377

Taylor, C. M., Birch, C. E., Parker, D. J., Dixon, N., Guichard, F., Nikulin, G., & Lister, G. M. S. (2013). Modeling soil moisture-precipitation feedback in the Sahel: Importance of spatial scale versus convective parameterization. *Geophysical Research Letters*, *40*(23), 6213–6218. https://doi.org/10.1002/2013GL058511

Tuttle, S., & Salvucci, G. (2016). Empirical evidence of contrasting soil moisture–precipitation feedbacks across the United States. *Science*, *352*(6287), 825–828. https://doi.org/10.1126/science.aaa7185

Xia, Y., Mitchell, K., Ek, M., Sheffield, J., Cosgrove, B., Wood, E., Luo, L., Alonge, C., Wei, H., Meng, J., Livneh, B., Lettenmaier, D., Koren, V., Duan, Q., Mo, K., Fan, Y., & Mocko, D. (2012). Continental-scale water and energy flux analysis and validation for the North American Land Data Assimilation System project phase 2 (NLDAS-2): 1. Intercomparison and application of model products. *Journal of Geophysical Research: Atmospheres*, *117*(D3). https://doi.org/10.1029/2011JD016048

Yang, K., Chen, Y., He, J., Zhao, L., Lu, H., Qin, J., Zheng, D., & Li, X. (2020). Development of a daily soil moisture product for the period of 2002–2011 in Chinese mainland. *Science China Earth Sciences 2020 63:8*, *63*(8), 1113–1125. https://doi.org/10.1007/S11430-019-9588-5

Yang, Z.-L., Niu, G.-Y., Mitchell, K. E., Chen, F., Ek, M. B., Barlage, M., Longuevergne, L., Manning, K., Niyogi, D., Tewari, M., & Xia, Y. (2011). The community Noah land surface model with multiparameterization options (Noah-MP): 2. Evaluation over global river basins. *Journal of Geophysical Research*, *116*(D12), D12110. https://doi.org/10.1029/2010JD015140

Zeng, X., Liu, J., Ma, Z., Song, S., Xi, C., & Wang, H. (2010). Study on the effects of land surface heterogeneities in temperature and moisture on annual scale regional climate simulation. *Advances in Atmospheric Sciences*, *27*(1), 151–163. https://doi.org/10.1007/S00376-009-8117-4/METRICS

Zhang, X., Niu, G.-Y., Elshall, A. S., Ye, M., Barron-Gafford, G. A., & Pavao-Zuckerman, M. (2014). Assessing five evolving microbial enzyme models against field measurements from a semiarid savannah-What are the mechanisms of soil respiration pulses? *Geophysical Research Letters*, *41*(18), 6428–6434. https://doi.org/10.1002/2014GL061399